A Polarized Photobleaching Study of DNA Reorientation in Agarose Gels†

Bethe A. Scalettar,*,‡ Paul R. Selvin,‡,§ Daniel Axelrod,∥ Melvin P. Klein,‡ and John E. Hearst‡,⊥

Chemical Biodynamics Division, Lawrence Berkeley Laboratory, Berkeley, California 94720, Department of Physics and Department of Chemistry, University of California, Berkeley, California 94720, and Department of Physics, University of Michigan, Ann Arbor, Michigan 48109

Received October 18, 1989; Revised Manuscript Received January 19, 1990

ABSTRACT: Polarized fluorescence recovery after photobleaching (pFRAP) has been used to study the internal dynamics of relatively long DNA molecules embedded in gels that range in concentration from 1% to 5% agarose. The data indicate that, even in very congested gels, rapid internal relaxation of DNA is largely unhindered; however, interactions with gel matrices apparently do perturb the larger amplitude, more slowly (microseconds to milliseconds) relaxing internal motions of large DNAs. The relationship between this work and recent studies which indicate that internal motions of DNA play an important role in the separation achieved with pulsed-field gel electrophoresis techniques is discussed. The polarized photobleaching technique is also analyzed in some detail. In particular, it is shown that "reversible" photobleaching phenomena are probably related to depletion of the ground state by intersystem crossing to the triplet state.

Gel electrophoresis is an effective and widely exploited method for separating molecules on the basis of their size. Because the technique plays such an important role in the isolation and characterization of DNA, the mechanisms by which it yields separation have been the subject of extensive experimental [reviewed by Cantor et al. (1988)] and theoretical [see, among others, Deutsch (1988), Lerman and Frisch (1982), Lumpkin et al. (1985), and Noolandi et al. (1989)] study. Unfortunately, to date, many of the molecular details of DNA migration during electrophoresis remain uncharacterized, although, in a general sense, it is known that separation is achieved because interactions between the gel matrix and the DNA impart a size dependence to the electrophoretic mobility [reviewed by Cantor et al. (1988)]. Here we have undertaken a study of the Brownian reorientation of DNAs in gels in an attempt to characterize, experimentally, the mechanisms by which DNA molecules interact with gel matrices.

Translation of DNA in gels has been studied by following the field-induced motion of a "band", or population, of DNA molecules as a function of time. For example, this band migration technique has been used to show that the constant-field gel electrophoretic mobility of DNA in agarose generally increases with field strength and temperature, and generally decreases with molecular weight, gel concentration, and ionic strength (Hervet & Bean, 1987). Analogous studies of DNA migration in agarose under the influence of a pulsed electric field have demonstrated that molecular weight, gel concentration, temperature, and electric field strength have the same qualitative effects on the pulsed-field electrophoretic mobility [see Mathew et al. (1988) and companion papers].

Video microscopic techniques that permit visualization of individual long DNAs have recently revolutionized understanding of DNA motion in gels (Smith et al., 1989; Schwartz & Koval, 1989; Houseal et al., 1989). The microscopic approach has shown that, in the absence of an applied field, large DNAs look like random coils that have been more or less immobilized by their interactions with the gel (1.5% agarose) matrix (Smith et al., 1989). However, when an electric field is turned on, the DNA begins to elongate and migrate in the direction of the applied field. These, and additional, observations have provided a unique picture of the translational and overall reorientational motions of DNAs in gels.

Several recent experimental observations have spurred interest in study of the internal dynamics of DNA in congested systems such as gels and concentrated DNA solutions. For example, studies of very concentrated liquid-crystalline DNA solutions have demonstrated that interactions between DNA molecules can have dramatic effects on the internal motions of DNA (Rill et al., 1983). It has also become apparent that the internal modes of DNA probably play an important role in the separation achieved with modern electrophoretic methods, such as field inversion electrophoresis (Carle et al., 1986; Noolandi et al., 1989). Unfortunately, to date, there have been relatively few reported studies of the internal dynamics of DNA in congested solutions.

The more rapidly relaxing, smaller amplitude internal dynamics of DNA can, and must, be detected with techniques that have greater temporal resolution than video microscopy. Here we have conducted a systematic study of the internal motions of DNA molecules in agarose gels with such a spectroscopic technique, polarized fluorescence recovery after photobleaching (pFRAP)[1] (Velez & Axelrod, 1988; Scalettar et al., 1988). [Photobleaching techniques have also recently been used to measure electrophoretic mobilities of DNA molecules in agarose gels (Chu et al., 1989)]. The relatively new pFRAP technique is well-suited for our purposes because it allows signal detection with small quantities of sample and because it can be used to detect motions that relax in a time

† This work was supported by NIH Grants GM41911 (J.E.H. and M.P.K.) and NS14565 (D.A.), by NSF Grant DMB8805296 (D.A.), by the Office of Energy Research, Office of Health and Environmental Research of DOE, under Contract DE AC03-76SF00098, and by an appointment (B.A.S.) to the Alexander Hollaender Distinguished Postdoctoral Fellowship Program supported by DOE and administered by Oak Ridge Associated Universities.

* Address correspondence to this author at the Department of Cell Biology and Anatomy, University of North Carolina, Chapel Hill, NC 27599-7090.

‡ Lawrence Berkeley Laboratory.

§ Department of Physics, University of California.

∥ Department of Physics, University of Michigan.

⊥ Department of Chemistry, University of California.

[1] Abbreviations: pFRAP, polarized fluorescence recovery after photobleaching; LMT, low melting temperature; bp, base pair(s); FIGE, field inversion gel electrophoresis.

0006-2960/90/0429-4790$02.50/0 © 1990 American Chemical Society

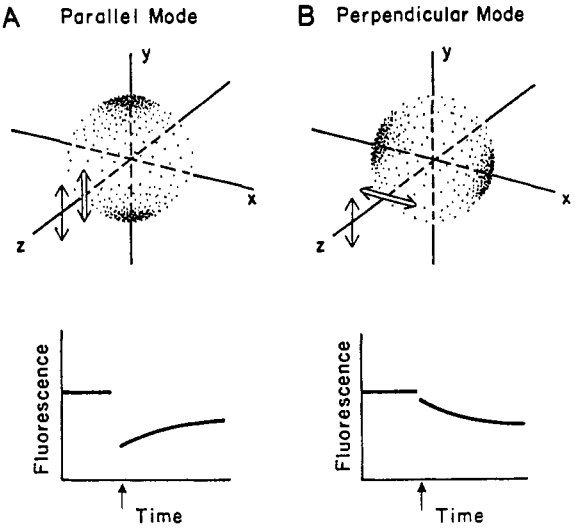

FIGURE 1: Schematic representation of the parallel and perpendicular mode pFRAP experiments. The bleach beam (double arrow) first creates an orientationally asymmetric fluorophore distribution in the sample. Fluorescence excited by the probe beam (single arrow) is then used to follow the temporal evolution of this initial distribution. In a parallel mode experiment (A), the probe beam initially excites a population of bleached dye, and, thus, at $t = 0$ (immediately after the bleach), the signal is small. The postbleach fluorescence then recovers with time as molecules rotate, and the bleached dye thus becomes more uniformly distributed over angular space. In a perpendicular mode experiment (B), on the other hand, the probe beam initially excites a population of unbleached dye, and, thus, at $t = 0$, the signal is relatively large. Moreover, *if* reorientational motion alone leads to a return of an isotropic angular distribution of dye, the perpendicular mode fluorescence will decay with time.

regime (≥ 5 μs) that is appropriate for the system of interest. Moreover, pFRAP and fluorescence methods in general are selective labeling techniques, and thus our pFRAP signal originates purely from the DNA component of the agarose/DNA system. [Alternative optical methods, such as phosphorescence emission (Jovin et al., 1981), could also, in principle, be used to study the system of interest here.] In this work, we also describe in detail some characteristics of the photophysics of photobleaching that we have recently deduced from our studies. In particular, we will provide a plausible molecular mechanism for the reversible photobleaching phenomenon that we have previously described (Velez & Axelrod, 1988; Scalettar et al., 1988).

THEORY

Reorientational Relaxation in pFRAP Experiments. Here we present a sketch of the way in which reorientational motion is detected in pFRAP experiments; more detailed descriptions of the technique may be found elsewhere (Velez & Axelrod, 1988; Scalettar et al., 1988). In a pFRAP experiment, a brief (microsecond) pulse of intense, polarized light is used preferentially to bleach (render nonfluorescent) some of those dye molecules in a sample whose absorption moments have a component parallel to the polarization of the light at the time of the bleach. This "polarized photobleaching" produces an anisotropic angular distribution of fluorophore in the sample (see Figure 1A). A much less intense ($\approx 1/5000$) polarized probe/observation beam is then directed onto the sample. This observation beam ideally does little further bleaching; it merely produces a postbleach fluorescence signal which can be used to monitor the return of an isotropic angular distribution of dye.

Rotational diffusion will cause the anisotropy in the angular distribution of fluorophore to dissipate. During the observation period, random Brownian forces will cause the orientational populations of bleached and unbleached dye to redistribute themselves until the postbleach angular dye distribution eventually again becomes isotropic.

Nonreorientational Relaxation in pFRAP Experiments. We find that, on the microsecond time scale, rotational motion is not the only phenomenon that contributes to the time dependence of the pFRAP signal (Velez & Axelrod, 1988; Scalettar et al. 1988). The observations that led us to draw this conclusion are summarized in Figures 1, 2A, and 3A. Assume for the moment that all bleaching is irreversible, i.e., pFRAP data reflect only rotation. [Irreversible bleaching probably takes place when an excited dye in the singlet state crosses into the triplet state and then reacts irreversibly with oxygen (Foote, 1968; Geacintov & Brenner, 1989).] If this situation obtains, pFRAP data will have the characteristics shown in Figure 1, when the probe and bleach beam are either parallel (parallel mode) or perpendicular (perpendicular mode) to one another. In particular, in Figure 1 it is noted that a pure rotational relaxation will cause the perpendicular mode pFRAP signal, $F_\perp(t)$, to decay with time. It is also noted there that the following relationship is expected to hold: $F_0 - F_\perp(0) \leq F_0 - F_\parallel(0)$; here, F_0 is the prebleach signal, $F_\perp(0)$ is the postbleach signal in the perpendicular mode immediately after bleaching, and $F_\parallel(0)$ is the parallel mode signal immediately after the bleach. If one then looks at typical pFRAP experimental data (see, e.g., Figures 2A and 3A), it is seen that $F_\perp(0)$ and $F_\parallel(0)$ differ in the manner expected; however, $F_\perp(t)$ recovers with time and, therefore, clearly does not have the temporal characteristics of a purely rotational process. Hence, we have concluded that rotational motion and another relaxation process simultaneously contribute to pFRAP data.

In subsequent sections, the additional relaxation is attributed to *reversible* bleaching. Moreover, it is shown there that reversible bleaching probably represents a photophysical relaxation from a triplet state. The distinction between irreversible and reversible bleaching thus seems to be that a reversibly bleached dye fails to react irreversibly with oxygen. We focus attention on reversible bleaching because under our experimental conditions the signal comes predominantly from a reversible bleach. In standard translational photobleaching experiments, the signal comes predominantly from an irreversible bleach.

Since the time dependences of $F_\parallel(t)$ and $F_\perp(t)$ are determined by rotational motion and reversible photobleaching, it is necessary to devise a method of isolating the reorientational component of the pFRAP relaxation. It has been shown (Velez & Axelrod, 1988) that this can be accomplished by constructing an anisotropy function, $r_b(t)$, from the data obtained in parallel and perpendicular mode pFRAP experiments. Specifically, if the quantity

$$r_b(t) = [\Delta F_\parallel(t) - \Delta F_\perp(t)]/[\Delta F_\parallel(t) + 2\Delta F_\perp(t)] \quad (1)$$

is calculated, the time dependence of $r_b(t)$ is determined only by reorientational motion. Here $\Delta F_\parallel(t) = F_0 - F_\parallel(t)$ and $\Delta F_\perp(t) = F_0 - F_\perp(t)$. In general, $r_b(t)$ will decay from some positive initial value, $r_b(0)$, to zero, at a rate which is determined by the rate at which the molecules in the sample rotate. It has been demonstrated that the temporal dependence of $r_b(t)$ provides an accurate measure of rotational relaxation rates in well-defined control samples consisting of spherical beads (Velez & Axelrod, 1988).

We will focus attention on two types of parameters that can be extracted from the pFRAP anisotropy. These are the time constant(s), τ_i, associated with the rate at which $r_b(t)$ decays to zero and the initial value of the anisotropy, $r_b(0)$. This latter quantity gives a measure of the extent of rapid (≤ 5 μs) motion

in the sample. Specifically, $r_b(0)$ is large and positive (4/7 = 0.57) if the molecules are immobile during the bleach pulse and *zero* if the molecules in the sample reorient completely on the time scale of the bleach. If the experimental value of $r_b(0)$ lies between these two extrema, the molecules have undergone some restricted amplitude motion during the bleach.

As mentioned above, the time constant or constants are related to the rate at which the larger amplitude reorientational motions relax. If the molecules in the sample possess some relatively simple shape, the τ_i's can be quantitatively related to specific parameters, such as rotational diffusion coefficients. However, the molecules under study here exhibit a dynamics that is very complex; hence, we will usually just calculate *one* effective exponential relaxation rate and see how this effective τ changes as the sample is manipulated.

Finally, we note that in our previous work (Scalettar et al., 1988) we used a simple ratio, $R(t) = \Delta F_\perp(t)/\Delta F_\parallel(t)$, to isolate the rotational component of the pFRAP recovery. The information contained in the anisotropy and ratio is equivalent, and, in fact, the two quantities are easily interchanged, i.e., $r_b(t) = [1 - R(t)]/[1 + 2R(t)]$. We will henceforth report $r_b(t)$ because its definition is analogous to that of the fluorescence depolarization anisotropy. It is important to note, however, that the pFRAP and fluorescence depolarization experiments probe a somewhat different set of time-dependent angular averages and, therefore, there are subtle differences between the pFRAP and fluorescence depolarization anisotropies; this point has been discussed in detail in our past work (Velez & Axelrod, 1988; Scalettar et al., 1988).

Preliminary Characterization of Reversible Photobleaching. We have made some attempt here to characterize the mechanisms that underlie reversible photobleaching of dyes. It had previously been suggested that reversible photobleaching might represent an intersystem crossing of an excited singlet dye into a triplet state (Velez & Axelrod, 1988). Such a mechanism seemed reasonable because when a dye molecule exists in a triplet state it will not absorb light from the probe beam, and hence, during this time, it will appear to be bleached. (Triplet to triplet absorption at the excitation wavelength is expected to be minimal.) Moreover, if the triplet state can decay back to the ground singlet state, the "bleach" clearly will not be permanent but will have a component of reversibility to it.

We have now begun to test the triplet hypothesis by looking at the oxygen dependence of the photophysical recovery time. Since triplet lifetimes lengthen markedly in deoxygenated samples, the time constant associated with reversible photobleaching should increase dramatically in deoxygenated solutions if triplet states are involved in the photophysical recovery processes. As demonstrated under Results, the predicted oxygen effect is indeed observed. Hence, we currently believe that the *reversible* photobleaching seen in pFRAP experiments is very analogous to the "singlet state depletion" described by Johnson and Garland (1982), Hogan et al. (1982), and Yoshida and Barisis (1986).

Although one of the attractive features of polarized photobleaching is that it can be used to study slow rotational motion in samples that are not deoxygenated, it can still be advantageous to deoxygenate if the sample is not damaged by removal of O_2. In general, deoxygenation will improve the signal-to-noise ratio obtained from pFRAP data that relax characteristically in the microsecond time domain. In a pFRAP experiment, the signal-to-noise ratio of the anisotropy improves as the depth of bleach, $[F_0 - F_\parallel(0)]/F_0$, and reversible relaxation time increase. If the photophysical recovery time is lengthened (by removing O_2), and $F_\parallel(t)$ and F_0 do not, therefore, approach one another as quickly, the signal-to-noise ratio obtained at long times will improve. For this reason, all gel data described here were obtained from deoxygenated samples; however, it was verified that the parameters extracted from the data were not influenced by this procedure.

Materials and Methods

Oxygenation and Deoxygenation of DNA Samples. Samples that were to be oxygenated/deoxygenated were manipulated in an oxygen/nitrogen-saturated glovebag. Buffers were oxygenated/deoxygenated by bubbling the appropriate gas through them for approximately 15 min. Deoxygenated agarose samples were held in standard quartz coverslip sample holders, which we rendered sufficiently air-tight simply by sealing all interfaces with vaseline or vacuum grease. The DNA solutions used in the photophysics studies were held in air-tight sample chambers that were constructed from 500-μL Eppendorf tubes which were slit (in the transverse direction) at the tip with a razor; the slit end was then glued to a quartz coverslip with epoxy resin. Since the photophysical recovery time is a very sensitive function of oxygen concentration, we could assay for air leaks simply by monitoring the time dependence of the photophysical recovery rate.

DNA, Fluorophores, and Sample Labeling. An 18 base pair oligomer was synthesized in our laboratory on a DNA synthesizer (Biosearch) and then purified on a standard polyacrylamide gel. pBR322, primarily in the closed circular form, was purchased from Bethesda Research Laboratories. Finally, linear phage λ DNA was also obtained from Bethesda Research Laboratories.

DNA was labeled with ethidium bromide (Sigma Chemicals) by combining the appropriate amount of stock DNA with an ethidium bromide solution and then allowing the dye to intercalate in the dark; approximately 1 dye molecule was bound per 200 base pairs of phage λ or pBR322 DNA. On the average, one dye was bound to each oligomer.

Preparation of DNA Samples Used in Photophysics Studies. Three solutions of ethidium bromide stained phage λ DNA were prepared at 300 μg/mL DNA. One was kept in equilibrium with the atmosphere; two other identical samples were prepared by bubbling either nitrogen or oxygen through the buffer. These latter two samples are referred to as deoxygenated and oxygenated, respectively.

Preparation of DNA Gels. DNA gels were prepared as follows. Several milliliters of a concentrated low-melting-temperature (LMT) agarose (Sigma Chemicals lot no. 115F-0666, M_r 0.08) solution, buffered with 0.089 M Tris, 0.089 M boric acid, and 0.0032 M EDTA, pH 8.3, were prepared by stirring and warming on a hot plate. Simultaneously, a solution of ethidium bromide stained DNA was heated in a water bath on the hot plate. The volume of this DNA solution and the concentration of agarose in the gel were adjusted to ensure that when the two solutions were combined the agarose concentration (w/v) would have the final desired value; the final DNA concentration in all the samples was 80 μg/mL. The gel and DNA were combined and gently mixed (not stirred) until the sample was homogeneous. We, in fact, chose to prepare our samples from LMT agarose because the gels with lower melting temperature solidified sufficiently slowly to permit us to mix them thoroughly. Before beginning an experiment, these gel/DNA mixtures were warmed (melted), and an aliquot was placed on a quartz coverslip and allowed to solidify in a nitrogen-saturated glovebag. After the stocks had been subjected to several warming and cooling cycles, we tested for degradation of the DNA by running an electrophoretic gel. No degradation was detected.

Description of the Apparatus and pFRAP Experimental Methods. The pFRAP apparatus has been described in detail previously (Velez & Axelrod, 1988). The microscope stage is under the control of a microstepping motor. Hence, after each round of bleach and probe, the stage is horizontally translated about 3 μm (which is the approximate beam diameter). Translation of the stage ensures that no point on the sample is exposed to bleaching light more than once.

For all of the agarose experiments, we used a 5-μs bleaching pulse. The prebleach and postbleach fluorescence signals were recorded for 50 and 200 (5 μs) time points, respectively. The standard prebleach fluorescence count rate ranged between 50 000 and 100 000 counts/s. The signal needed to be averaged approximately 100 000 times (for several hours) to achieve a good signal-to-noise ratio.

The light intensity was adjusted to produce a 25–40% bleach in the sample; a larger bleach was avoided because $r_b(0)$ decreases when the bleach is deep (Velez & Axelrod, 1988). For our particular experimental setup, the desired bleach was produced when the laser (a 15-W Coherent argon ion) was run at 2-W output power on the 514.5-nm line. The beam was sometimes attenuated slightly, e.g., with an optical density 0.2–0.4 filter. It is worth noting that there is considerable loss of light as the beam travels from the laser to the microscope and, hence, only approximately 100 mW of power actually impinges on the sample. A 10× glycerine immersion objective with a numerical aperture of 0.5 was used to focus light onto the sample. Our calculations show that such experimental conditions lead to a negligible light-induced temperature rise in the sample (Velez & Axelrod, 1988; Scalettar et al., 1988).

Data Analysis. The fundamental experimental quantity of interest is the pFRAP anisotropy. The anisotropy was computed according to its definition from either the raw pFRAP data, $F_\parallel(t)$ and $F_\perp(t)$, or data that were given a five-point quadratic smooth (Savitzky & Golay, 1964).

Since we do not have a theoretical expression that relates the exact time dependence of the pFRAP anisotropy to the various relaxation modes of DNA (see Reorientation of pBR322 and Phage λ DNA in Agarose gels), we have chosen to fit $r_b(t)$ to a single decaying exponential function. Such a fit gives us an approximate quantitative measure of the average relaxation time and of the initial anisotropy and, in fact, was usually found to provide a reasonable description of the temporal dependence of the data. Nevertheless, there is no a priori reason to expect the $r_b(t)$'s reported here to decay as single exponentials. Curve fits were obtained by using a modified version of the program CURFIT (Bevington, 1969). This program uses all data points in obtaining the best-fit parameters; however, the "weight" attached to each data point is determined by the statistical significance it manifests in the individual recovery curves.

The individual recovery curves, and not the anisotropy function, are the experimentally relevant quantities when one is studying the reversible bleaching process. [Recall that $r_b(t)$ contains information only about rotation.] Moreover, the entire time dependences of $F_\parallel(t)$ and $F_\perp(t)$ can be attributed to photophysics if we independently verify that the associated anisotropy is zero. Such is the case for a dilute λ DNA solution. Photophysical data were analyzed by fitting the pFRAP curve, $F_\parallel(t)$, to a single recovering exponential function and associating the best-fit time constant with the reversible recovery time.

Results

Rotational Diffusion of Short Oligomers in Agarose Gels. The rotational diffusion of an 18 base pair oligomer in agarose was monitored with the pFRAP technique. Such an experiment allows us to follow the reorientation of a small DNA molecule in a matrix. In Figure 2A, the individual pFRAP curves, $F_\parallel(t)$ and $F_\perp(t)$, obtained from a 5% agarose/oligomer sample are shown. The two curves are essentially indistinguishable. The anisotropy computed from the data in Figure 2A is shown in Figure 2B; it is flat and zero over the entire time regime examined.

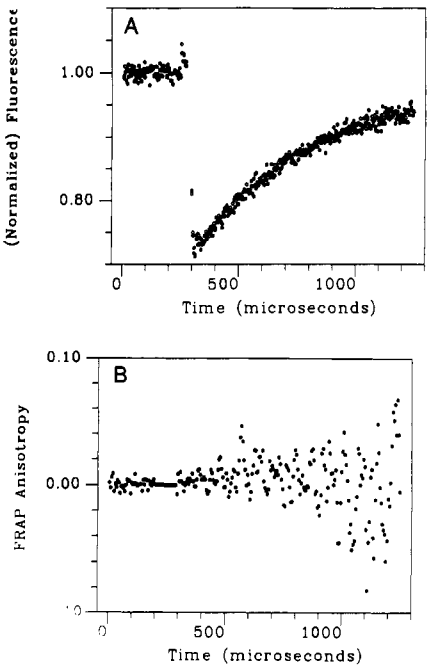

FIGURE 2: Polarized photobleaching curves (A) $F_\parallel(t)$ (closed circles) and $F_\perp(t)$ (open circles) obtained from an ethidium bromide stained oligomer embedded in a 5% agarose gel. The individual curves superimpose, and, hence, the numerator, $\Delta F_\parallel(t) - \Delta F_\perp(t)$, of the anisotropy function, $r_b(t)$, is zero over the entire time regime examined (B).

Rotational Diffusion of pBR322 in Agarose Gels. We were also interested in looking at the effects that interactions with gel matrices have on the reorientational motion of a typical circular DNA plasmid. The pFRAP data obtained from a sample consisting of the plasmid pBR322 (≈4000 bp) embedded in a 5% agarose gel are shown in Figure 3. For this larger DNA molecule, it is apparent that $F_\parallel(t)$ and $F_\perp(t)$ do differ. In particular, it is seen that the depth of bleach is slightly deeper in the parallel mode than in the perpendicular; therefore, we conclude that, in this sample, the DNA molecules have not completely reoriented at the end of the 5-μs bleaching pulse. The anisotropy function $r_b(t)$ computed from the data shown in Figure 3A is displayed in Figure 3B. The magnitude of the initial anisotropy is small, ≈0.02; the best-fit time constant is 540 μs.

Rotational Diffusion of Phage λ DNA in Agarose Gels. We have studied the reorientational relaxation of phage λ DNA (≈50 000 bp) in agarose as a function of gel concentration. Dynamics in gels that were 1%, 2%, 3%, 4%, and 5% by weight was monitored. These studies allowed us to follow the effects that interactions with gel matrices have on the various relaxation modes of relatively long, linear DNA molecules.

The anisotropy obtained from a sample consisting of phage λ DNA in 5% agarose is shown in Figure 4A. Two other anisotropy functions, corresponding to agarose concentrations of 3% and 1%, are shown, for comparative purposes, in Figure 4B, C. Finally, the best-fit time constants and initial anisotropies obtained from all five samples are summarized in Figures 5 and 6. It is seen that both the time constant and

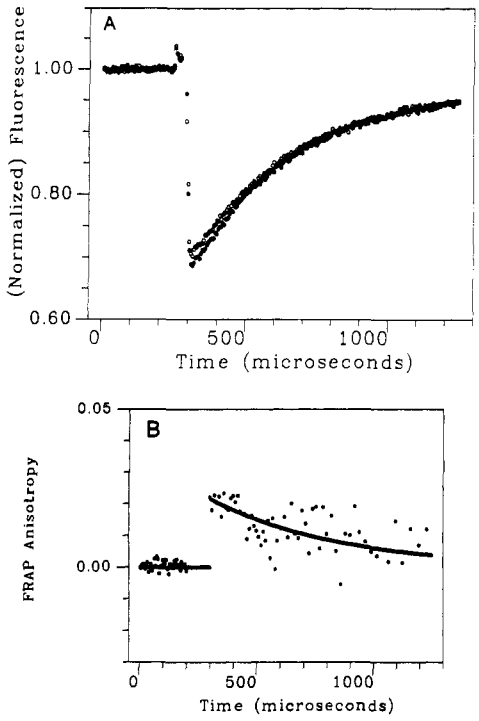

FIGURE 3: Parallel and perpendicular mode pFRAP curves (A) and associated anisotropy (B) obtained from a sample consisting of ethidium bromide stained pBR322 embedded in 5% agarose. In this gel sample, the bleach is deeper in the parallel mode (closed circles) than in the perpendicular mode (open circles). The initial anisotropy is small, and we, therefore, conclude that pBR322 undergoes a substantial amount of rapid, unresolved motion during the bleaching pulse. The temporal decay of $r_b(t)$ then allows us to monitor the evolution of the more slowly relaxing reorientational motions of the DNA. Note that although the data were collected at 5-μs sample intervals (bins), the anisotropy functions displayed in Figures 3 and 4 were obtained by adding together neighboring bins (for the long time data points only); this procedure improves the signal-to-noise ratio at long times.

$r_b(0)$ increase systematically as the agarose concentration is changed.

Oxygen Sensitivity of Photophysical Recovery. In Figure 7, we see that the photophysical recovery time is a very sensitive function of the oxygen concentration in the sample. Specifically, if a sample of ethidium bromide stained phage λ DNA is saturated with oxygen, the photophysical recovery time is 70 μs. If an identical sample is in equilibrium with the atmosphere, the time constant is 140 μs. Finally, upon deoxygenation, the recovery time increases to 1.8 ms. Note also that the depth of bleach is a monotonically decreasing function of O_2 concentration; in fact, if one compares oxygenated and deoxygenated DNA solutions, it is seen that a given light intensity will produce a bleach that is substantially deeper in the sample that lacks oxygen.

Discussion

Rotational Diffusion of Short DNA Fragments in Agarose Gels. The agarose gels studied here are composed predominantly of buffer. Therefore, over small distance scales, a DNA molecule should be interacting primarily with an aqueous solution, and the forces that act on it will largely be Brownian in origin. Indeed, if the effective pore size of the gel is much larger than the dimensions of the DNA, it seems likely that the rotational motion exhibited by the DNA will not differ much from that of an identical molecule which is tumbling unimpeded in solution under the influence of Brownian torques.

Stellwagen (1985) has conducted a systematic study of the Brownian rotational diffusion of DNA restriction fragments (622–2936 bp in length) in agarose gels using the transient

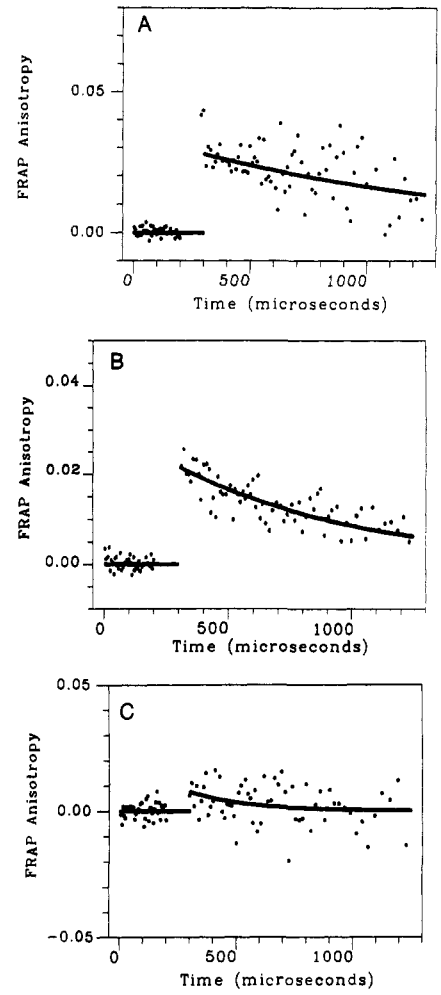

FIGURE 4: Anisotropy functions obtained from samples consisting of phage λ DNA embedded in 1%, 3%, and 5% agarose. The DNA in the most dilute gel (C) exhibited essentially no anisotropy at the end of the bleaching pulse; in contrast, both the 5% (A) and 3% (B) agarose/DNA samples yielded nonzero values for $r_b(0)$. Visual inspection of the data shows that the temporal decay of residual anisotropy was more rapid in the 3% gel than in the most dense gel.

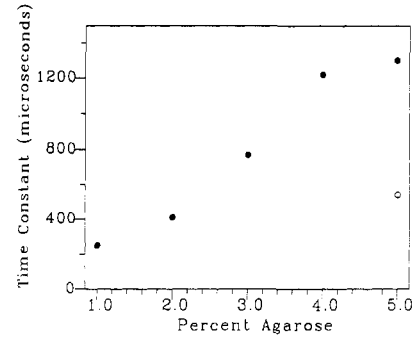

FIGURE 5: Best-fit time constants obtained from the five phage λ DNA samples (closed circles) and the pBR322 sample (open circle). The phage λ DNA time constant increases monotonically with agarose concentration. The pBR322 time constant is somewhat smaller than its λ DNA analogue. Note that each of the phage λ DNA and pBR322 experiments was repeated at least once and that reproducibility was quite good. The 1% agarose data point fitting parameters could not be determined very precisely.

electric birefringence technique [see also Wijmenga and Maxwell (1986) for related work]. The birefringence data do indeed indicate that the longest detected relaxation mode is unperturbed by the presence of a gel if the median gel pore diameter exceeds the hydrodynamic length of the DNA; however, interactions with the matrix markedly slow this re-

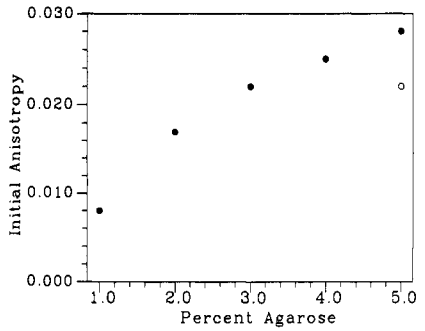

FIGURE 6: Best-fit initial anisotropies obtained from the five λ DNA samples and the pBR322 sample. For the λ DNA gels, the initial anisotropy increases with agarose concentration. Symbols are defined in Figure 5.

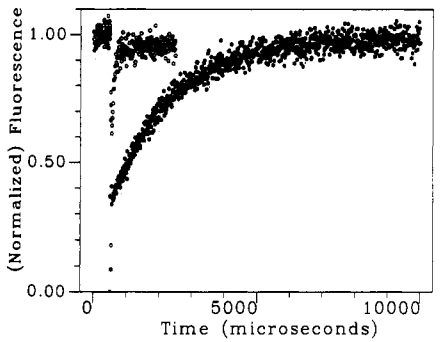

FIGURE 7: Photophysical recovery data obtained from a solution of ethidium bromide stained phage λ DNA. Only parallel mode curves, $F_{\parallel}(t)$, are shown. An oxygenated solution yielded the upper, more rapidly recovering data (open circles); a deoxygenated sample produced the lower, more slowly relaxing data (closed circles). Data corresponding to atmospheric conditions are not shown. Note that the samples differ dramatically in the rate at which their signal recovers and in their apparent susceptibility to bleaching. We have also observed that the irreversible component, $F_0 - F_{\parallel}(\infty)$, of the pFRAP bleach is slightly larger in oxygenated samples. This latter result reaffirms the fairly well-documented (Foote, 1968; Magde et al., 1974) idea that oxygen is also involved in the molecular events that lead to irreversible bleaching.

laxation mode if the median pore diameter is smaller than the hydrodynamic length.

The oligomer/agarose sample studied here has properties that would lead us to expect it to approach the freely tumbling limit. An 18 base pair oligomer is effectively a rigid rod with a length of ≈61 Å. Moreover, the pore sizes of agarose gels that are a few percent by weight LMT agarose range between 250 and 1000 Å (Griess et al., 1989; Serwer, 1983). Hence, our oligomer is indeed much smaller than are the pores of the gel.

One can easily calculate, from the Broersma formulas (Broersma, 1960), the long-axis and end-over-end rotational diffusion coefficients for a rigid rod of 61 Å in length. The values obtained are 3×10^7 and 2×10^6 s^{-1}, respectively. The associated long-axis and end-over-end relaxation times are on the order of a few tens and a few hundreds of nanoseconds, respectively. These correlation times are so short that unless interactions between the oligomer and the matrix had markedly impeded the rotational motion of the 18-mer, the pFRAP anisotropy obtained at the end of a 5-μs bleaching pulse should be zero. This is indeed what we have observed. This oligomer experiment thus serves as a control on our λ DNA and pBR322 work; in particular, it serves as a test for instrumentally introduced anisotropy in the data. The oligomer result demonstrates, for example, that the intensities of the bleaching light in the parallel and perpendicular modes are the same. If these two intensities were not essentially equal, a rapidly tumbling (on the microsecond time scale) molecule would yield a static, nonzero, anisotropy.

Reorientation of pBR322 and Phage λ DNA in Agarose Gels. Longer DNA molecules, like phage λ DNA, are semiflexible macromolecules that undergo, in dilute solution, both twisting and bending motions, rotations of internal segments, and entropically driven coil deformations (Shibata et al., 1985; Langowski et al., 1985; Hagerman, 1988). It would, therefore, be very useful to know how the pFRAP anisotropy evolves in time if reorientational relaxation in the system has it origins in twisting and bending dynamics. Unfortunately, in this case, the analysis of the time dependence of the angular quantities that contribute to common spectroscopic signals has proven to be a formidable theoretical problem. For example, although twisting and coil motions have been successfully incorporated into the description of many types of time-resolved experiments, bending dynamics has been analyzed only within the confines of approximate theories (Shibata et al., 1985; Barkley & Zimm, 1979).

In discussing our results for the longer DNAs, we thus do not attempt to present a rigorous theoretical analysis of the pFRAP data. We have opted, instead, to describe semiquantitatively the approximate amplitudes and time scales associated with *some* of the more rapidly (twisting) and slowly (coil) relaxing motions exhibited by long DNA molecules and, then, to discuss how these motions may be affected by interactions with gel matrices. It should also be mentioned, in this context, that some of the gel-induced effects that we have detected may arise when DNA molecules become entangled on the agarose (Smith et al., 1989). In the analysis that follows, we will, nevertheless, focus primarily on molecules that are interacting transiently with the matrix.

We have seen that samples consisting of relatively large DNA molecules, embedded in concentrated agarose gels, exhibit anisotropy (unlike the oligomer sample discussed above, and unlike a dilute solution of phage λ or pBR322 DNA). It is, however, important to note that the magnitude of the anisotropy that remains in our pBR and λ DNA gels, at the end of the bleach, is quite small. Therefore, we conclude that DNA molecules embedded in gels undergo a substantial amount of reorientational motion on time scales shorter than 5 μs. This conclusion is to be contrasted with the observations made by Smith et al. (1989) when they used video techniques to monitor the Brownian dynamics of phage λ DNA in gels. At the level of resolution that is achieved with video cameras, λ DNA appears to be immobile in a gel. In fact, however, the DNA is apparently free to undergo many small-scale reorientational motions, even in very congested gels.

Since the pFRAP data indicate that many of the more rapidly relaxing internal motions of longer DNA molecules are not damped out in gels, it is worthwhile to review briefly what is known about the internal dynamics of DNA in noninteracting solutions. We can then try to understand the origin of the small, but nonzero, initial pFRAP anisotropies detected here by extrapolating from what has been learned about DNA motion in dilute solution.

A large body of data support the idea that DNA molecules undergo nanosecond twisting motions about their long axis [reviewed by Shibata et al. (1985)]. Thus, an important measure of the amount of rapid motion that might take place in the gel samples is the mean squared twist angle of a subunit (labeled j) in the middle of the DNA, $\langle \theta_j(t)^2 \rangle$. If we extend the intermediate zone somewhat beyond its domain of validity, the twist can be calculated as a function of time from the formula (Allison et al., 1982)

$$\langle \theta_j(t)^2 \rangle = 2k_B T(t/\pi\alpha\gamma)^{1/2} \quad (2)$$

Here $\alpha = 3.8 \times 10^{-12}$ dyn·cm is the twisting rigidity, $\gamma = 6.15 \times 10^{-23}$ dyn·cm·s is the friction factor for rotation of a DNA subunit about its z axis, k_B is Boltzmann's constant, and $T = 293$ K is the temperature. From eq 2, we calculate that at the end of a 5-μs bleaching pulse $\langle \theta_j(t)^2 \rangle^{1/2} = 148°$. Since it is probably reasonable to assume that DNA will still twist locally in a gel, the above calculation shows that there will be a considerable amount of twist-induced depolarization during the bleach and that the initial anisotropy is thus likely to be small.

Local twisting of DNA leads to reorientation about only one axis and will not, in general, totally depolarize the sample. The DNA must exhibit other, e.g., transverse, motions if the anisotropy is to decay completely. We will now show that gel/DNA interactions are perturbing some of these motions of DNA and that this perturbation probably gives rise to the relatively long-lived anisotropy decays detected here.

We now focus on understanding why the initial pFRAP anisotropy is nonzero. We know (data not shown) that if phage λ or pBR322 DNA is suspended in solution at 80 μg/mL, $r_b(0)$ is zero; hence, we assume that interactions with the agarose somehow inhibit motions of long DNA molecules that would normally cause comparable dilute DNA solutions to depolarize during the bleaching pulse. Moreover, we feel that it is intuitively reasonable to assume that a lateral/transverse internal motion with an amplitude on the order of the gel pore size might be retarded by interactions with the agarose. We would like, therefore, to see which internal motions of the DNA are likely to lead to interactions with the gel and to lengthen the retention of anisotropy.

Transverse displacements of the DNA helix axis are frequently described in terms of a set of normal coordinate motions. For example, equations that are often used to describe the transverse internal dynamics of DNA (Rouse, 1953; Zimm, 1956; Harris & Hearst, 1966; Aragon & Pecora, 1985) yield normal mode solutions that give simple sinusoidal relationships between transverse displacement and contour length along the DNA. The Langevin relaxation time, τ_m [which is related, but generally not equal, to spectroscopic relaxation times (Langowski et al., 1985)], and the associated mean squared fluctuation amplitude, $\langle \delta_m^2 \rangle$, of a given mode, m, can be calculated, within the confines of certain models, from the approximate formulas (Fujime, 1971; Berne & Pecora, 1976)

$$\tau_m = 2R_g^2/\pi^2 m^2 D_0 \quad (3)$$

and

$$\langle \delta_m^2 \rangle = NR_g^2/6\pi^2 m^2 \quad (4)$$

Here R_g and D_0 are, respectively, the radius of gyration and the translational diffusion coefficient of a DNA molecule composed of $N + 1$ subunits, respectively. If the relaxation time and mean squared amplitude expressions are evaluated by using parameters appropriate for a molecule like phage λ DNA, it is found that

$$\tau_m = 50/m^2 \text{ ms} \quad (5)$$

and

$$\langle \delta_m^2 \rangle^{1/2} = 3000/m \text{ Å} \quad (6)$$

As noted under Rotational Diffusion of Short DNA Fragments in Agarose Gels, the pore sizes of 1–4% LMT agarose gels lie in the 250–1000-Å range (Serwer, 1983; Greiss et al., 1989). The normal mode analysis thus leads us to conclude that in, for example, a 4% LMT agarose gel, coil deformations associated with mode numbers 1–12 are likely to lead to interaction between a molecule like phage λ DNA and the agarose. Note that this calculation will probably underestimate the number of interacting modes because pore sizes represent the largest effective spacing between agarose strands. Normal modes 1–12 would, in noninteracting systems, relax components of the pFRAP anisotropy on time scales that are longer than about 100 μs. However, in regions of the gel in which the interstrand spacing is half the pore size, the highest order interacting modes would relax components of the pFRAP anisotropy on time scales of a few tens of microseconds. Thus, this very approximate argument leads us to conclude that anisotropy retention in a gel on the microsecond time scale could arise from gel-induced inhibition of lateral deformations of DNA molecules.

It is also worth noting that an approximately 10-μs reorientational relaxation has been detected in light scattering and dichroism experiments and has been attributed to end-over-end tumbling of persistence length segments of long DNAs (Schmitz & Schurr, 1973; Ding et al., 1972). Since the persistence length of DNA is about 600 Å, one would expect such a motion to be perturbed in gels whose pore sizes range between 250 and 1000 Å, such as those studied here. Inhibition of this end-over-end tumbling motion might also lead to the microsecond anisotropy retention detected in our studies.

Relationship to Electrophoretic Phenomena. We conclude our discussion of dynamics by commenting on the relationship between the experimental observations presented here and recent studies of the mechanisms that underlie the separation achieved with pulsed-field gel electrophoresis techniques. Several recent computer simulations of DNA migration under the influence of a pulsed field (Deutsch, 1988; Noolandi et al., 1989) suggest that interactions between gel matrices and the internal modes of DNA are a critical determinant of pulsed–electrophoretic separatory processes. For example, Noolandi et al. have been able to show that when internal motions of DNA are incorporated into simulations of mobility during field inversion gel electrophoresis (FIGE), the FIGE mobility has a minimum value at a certain pulse duration; this dramatic phenomenon has also been observed experimentally (Carle et al., 1986).

The experimental data presented here indicate that the internal motions of DNA which relax in the microsecond and millisecond time domain do indeed interact significantly with gels whose concentration is ≥1%. Moreover, we feel that it is likely that the interaction-induced effects detected here reflect interactions between transverse displacements of DNA conformation and the embedding matrix. Hence, future theoretical and experimental studies of the electrophoretic and Brownian dynamics of larger DNAs in gels should certainly continue to explore the relationship between internal motions of DNA and mobility in gels.

It is also worthwhile making one direct comparison between our pFRAP data and results obtained in studies of the agarose concentration dependence of the pulsed-field gel electrophoretic mobility. Specifically, we note that the initial value of the pFRAP anisotropy increases rapidly when the LMT agarose concentration is increased from 1% to 2%; in this same concentration regime, pulsed-field gel electrophoretic mobilities measured in standard agarose [which differs somewhat in pore size from LMT agarose (Serwer, 1983; Greiss et al., 1989)] begin to decrease rather dramatically [see Mathew et al. (1988) and companion papers]. It is interesting to speculate that these two phenomena are related to one another; one

might imagine, for example, that the same molecular interactions that hinder internal motions of DNA in a 2% agarose gel also fundamentally influence translational mobility in such a gel.

Physics of Reversible Photobleaching. Before the introduction of the microsecond polarized photobleaching technique, it was generally assumed that photobleaching was an irreversible reaction. [Indeed, the theory of translational FRAP is based on such an assumption (Axelrod et al., 1976).] However, the observations that we have presented here argue strongly that there is an oxygen-dependent mechanism that allows dye molecules to undergo temporary (reversible) "bleaching". Our results, although not definitive, are consistent with a reversible photobleaching mechanism that involves the excited singlet state crossing into a triplet state and then falling back into the ground (singlet) state. pFRAP monitors the fluorescence that is emitted when the excited singlet relaxes to the ground singlet; thus, a molecule that undergoes intersystem crossing to a triplet state and then relaxes back into the ground singlet state would appear to have been bleached and then to have recovered its ability to fluoresce. In such a scheme, the lifetime of this "reversible bleach" would be determined by the lifetime of the triplet.

It is this last feature of the photobleaching model that our experiments most critically address. It is well-known that triplet states are relaxed by dissolved oxygen; hence, triplet lifetimes increase markedly in deoxygenated solutions (Cantor & Schimmel, 1980). The relaxation reaction often is diffusion controlled, and its rate then is expected to be a linear function of oxygen concentration (Berkoff et al., 1986). Thus, if our model of the reversible photobleaching phenomenon is correct, we would expect the pFRAP photophysical recovery time, the inverse of the reaction rate, to be a monotonically decreasing function of oxygen concentration. This is indeed what we have observed experimentally. However, since we currently have measured pFRAP relaxation times at only three oxygen concentrations, it is somewhat difficult unambiguously to test for a linear dependence of reaction rate on O_2 concentration.

The dependence of the (reversible) bleach depth on oxygen concentration also supports the triplet hypothesis. If the scheme that we have outlined is correct, the reversible component of pFRAP is due to depletion of the singlet state by intersystem crossing to the triplet state, and, therefore, a pFRAP experiment that relies primarily on reversible bleaching is essentially equivalent to a singlet-state depletion experiment (Johnson & Garland, 1982; Yoshida & Barisas, 1986). In singlet-state depletion experiments, it is found that the depth of bleach increases in deoxygenated solutions (Johnson & Garland, 1982; Yoshida & Barisas, 1986). Since the reversible pFRAP bleach depth also exhibits this sort of oxygen dependence (see Figure 7), we again find consistency between the triplet scheme and our experimental observations.

It is helpful to compare the photophysical behavior of the putative triplet state seen in our pFRAP experiments to that of a putative ethidium triplet detected previously (Atherton & Beaumont, 1986, 1987). We first note that the deoxygenated triplet lifetime found here (1.8 ms) agrees well with the literature value. Moreover, both Atherton and Beaumont's data and our data indicate that ethidium bromide has an atypically long triplet lifetime in oxygenated samples; for example, Atherton and Beaumont find that the apparent rate constant for oxygen quenching of the ethidium triplet is 2 orders of magnitude smaller than typical rate constants for oxygen quenching of triplet states in homogeneous solution. Their speculation that intercalation of ethidium might serve to protect the triplet from interaction with O_2 seems reasonable.

A quantum efficiency for the intersystem crossing, ϕ, of ethidium bromide determined from our data can also be compared with a crude estimate ($\phi \approx 1\%$) made by Atherton and Beaumont. We can calculate ϕ if it is assumed that the bleach is due solely to crossover into the triplet state. In this case, ϕ is the bleach depth, B_D, divided by the number of photons absorbed per molecule during the bleaching pulse. A relatively straightforward application of Beer's law then shows that

$$\phi = (6 \times 10^{20}) B_D hc\pi\omega_0^2 / 2.3\epsilon\lambda P_0 t \qquad (7)$$

Here P_0 is the laser power, h is Planck's constant, c is the speed of light, λ is the wavelength of the laser light, t is the bleach duration, ϵ is the molar extinction coefficient of ethidium (in units of cm^{-1} M^{-1}), ω_0 is the beam spot size (in centimeters), and 6×10^{20} is a conversion factor. Note that ϕ is independent of dye concentration and path length. We find $\phi \approx 0.1\%$; the difference in the two values for ϕ probably stems from the approximate nature of both the Atherton and Beaumont calculation and the one presented here.

We close by comparing the relative merits of using fluorescence and phosphorescence emission to probe triplet states. Phosphorescence has an advantage over fluorescence because it is a signal that is measured "up from zero", rather than "down" from a prebleach level. However, phosphorescence emission efficiencies typically are small, and, thus, in many instances, fluorescence-detected singlet-state depletion methods, which depend only on the intersystem crossing efficiency, rather than the product of the intersystem and phosphorescence yields, are more sensitive than phosphorescence techniques. In fact, as Johnson and Garland point out, and our data demonstrate, a small intersystem efficiency is advantageous in a fluorescence experiment, if enough laser power is available to do the requisite "bleaching" (Johnson & Garland, 1982). We note finally, in this context, that very high light intensities are used to do bleaching in pFRAP; the intensities are not far removed from the regime in which two photon events could conceivably take place.

ACKNOWLEDGMENTS

We gratefully acknowledge helpful conversations with James Abney, Daniel Falvey, Nathan Hunt, Ariane McKiernan, Andrea Stout, Alan Waggoner, and Yifeng Yuan. We also thank Robert Fulbright, Edward Hellen, and Marisela Velez for assistance with software and the experimental apparatus, and Sharada Kumar for technical assistance. Finally, we thank Donald Burke-Aguerro and David Cook for being invaluable resources during the early stages of these studies.

Registry No. Agarose, 9012-36-6.

REFERENCES

Allison, S. A., Shibata, J., Wilcoxon, J., & Schurr, J. M. (1982) *Biopolymers 21*, 729–762.

Aragon, S. R., & Pecora, R. (1985) *Macromolecules 18*, 1868–1875.

Atherton, S. J., & Beaumont, P. C. (1986) *Photochem. Photobiol. 44*, 103–105.

Atherton, S. J., & Beaumont, P. C. (1987) *J. Phys. Chem. 91*, 3993–3997.

Axelrod, D., Koppel, D. E., Schlessinger, J. S., & Webb, W. W. (1976) *Biophys. J. 16*, 1055–1069.

Barkely, M. D., & Zimm, B. H. (1979) *J. Chem. Phys. 15*, 2991–3007.

Berkoff, B., Hogan, M., Legrange, J., & Austin, R. (1986) *Biopolymers 25*, 307–316.
Berne, B. J., & Pecora, R. (1976) *Dynamic Light Scattering*, pp 182–188, Wiley, New York.
Bevington, P. R. (1969) *Data Reduction and Error Analysis in the Physical Sciences*, pp 237–239, McGraw-Hill, New York.
Broersma, S. (1960) *J. Chem. Phys. 32*, 1626–1631.
Cantor, C. R., & Schimmel, P. R. (1980) *Biophysical Chemistry II*, pp 437, W. H. Freeman, San Francisco.
Cantor, C. R., Smith, C. L., & Mathew, M. K. (1988) *Annu. Rev. Biophys. Biophys. Chem. 17*, 287–304.
Carle, G. F., Frank, M., & Olson, M. V. (1986) *Science 232*, 65–68.
Chu, B., Wang, Z., & Wu, C. (1989) *Biopolymers 28*, 1491–1494.
Deutsch, J. M. (1988) *Science 240*, 922–924.
Ding, D., Rill, R. L., & Van Holde, K. E. (1972) *Biopolymers 11*, 2109–2124.
Foote, C. S. (1968) *Science 162*, 963–970.
Fujime, S. (1971) *J. Phys. Soc. Jpn. 31*, 1805–1808.
Geacintov, N. E., & Brenner, H. C. (1989) *Photochem. Photobiol. 50*, 841–858.
Griess, G. A., Moreno, E. T., Easom, R. A., & Serwer, P. (1989) *Biopolymers 28*, 1475–1484.
Hagerman, P. J. (1988) *Annu. Rev. Biophys. Biophys. Chem. 17*, 265–286.
Harris, R. A., & Hearst, J. E. (1966) *J. Chem. Phys. 44*, 2595–2602.
Hervet, H., & Bean, C. P. (1987) *Biopolymers 26*, 727–742.
Hogan, M., Wang, J., Austin, R. A., Monitto, C. L., & Hershkowitz, S. (1982) *Proc. Natl. Acad. Sci. U.S.A. 79*, 3518–3522.
Houseal, T. W., Bustamante, C., Stump, R. F., & Maestre, M. F. (1989) *Biophys. J. 56*, 507–516.
Johnson, P., & Garland, P. B. (1982) *Biochem. J. 203*, 313–321.
Jovin, T. M., Bartholdi, M., Vaz, W. L. C., & Austin, R. H. (1981) *Ann. N.Y. Acad. Sci. 366*, 176–196.
Langowski, J., Fujimoto, B. S., Wemmer, D. E., Benight, A. S., Drobny, G., Shibata, J. H., & Schurr, J. M. (1985) *Biopolymers 24*, 1023–1056.
Lerman, L. S., & Frisch, H. L. (1982) *Biopolymers 21*, 995–997.
Lumpkin, O. J., Dejardin, P., & Zimm, B. H. (1985) *Biopolymers 24*, 1573–1593.
Magde, D., Elson, E. L., & Webb, W. W. (1974) *Biopolymers 13*, 29–61.
Mathew, M. K., Smith, C. L., & Cantor, C. R. (1988) *Biochemistry 27*, 9204–9210.
Noolandi, J., Slater, G. W., Lim, H. A., & Viovy, J. L. (1989) *Science 243*, 1456–1458.
Rill, R. L., Hilliard, P. R., Jr., & Levy, G. C. (1983) *J. Biol. Chem. 258*, 250–256.
Rouse, P. E. (1953) *J. Chem. Phys. 21*, 1272–1280.
Savitzky, A., & Golay, J. E. (1964) *Anal. Chem. 36*, 1627–1639.
Scalettar, B. A., Selvin, P. R., Axelrod, D., Hearst, J. E., & Klein, M. P. (1988) *Biophys. J. 53*, 215–226.
Schmitz, K. S., & Schurr, J. M. (1973) *Biopolymers 12*, 1543–1564.
Schwartz, D. C., & Koval, M. (1989) *Nature 338*, 520–522.
Serwer, P. (1983) *Electrophoresis 4*, 375–382.
Shibata, J. H., Fujimoto, B. S., & Schurr, J. M. (1985) *Biopolymers 24*, 1909–1930.
Smith, S. B., Aldridge, P. K., & Callis, J. B. (1989) *Science 243*, 203–206.
Stellwagen, N. C. (1985) *J. Biomol. Struct. Dyn. 3*, 299–314.
Velez, M., & Axelrod, D. (1988) *Biophys. J. 53*, 575–591.
Wijmenga, S. S., & Maxwell, A. (1986) *Biopolymers 25*, 2172–2186.
Yoshida, T. M., & Barisas, B. G. (1986) *Biophys. J. 50*, 41–53.
Zimm, B. H. (1956) *J. Chem. Phys. 24*, 269–278.